International Symposium
On Turbulence and Shear Flow
Phenomena (TSFP-8)
August 28 - 30, 2013 Poitiers, France

CHARACTERISTICS OF FLOW OVER A CIRCULAR CYLINDER AT Re_d=140,000

Hyunsik Kim
School of Mechanical and Aerospace Engineering,
Seoul National University
Seoul 151-744, Korea
ukjaenim@snu.ac.kr

Jungil Lee
School of Mechanical and Aerospace Engineering,
Seoul National University
Seoul 151-744, Korea
deliciousair@gmail.com

Jooha Kim
School of Mechanical and Aerospace Engineering,
Seoul National University
Seoul 151-744, Korea
k-juha01@snu.ac.kr

Haecheon Choi
School of Mechanical and Aerospace Engineering,
Seoul National University
Seoul 151-744, Korea
choi@snu.ac.kr

ABSTRACT

In the present study, we conduct both numerical and experimental studies to investigate the characteristics of flow over a circular cylinder at Re_d = 140,000, where Re_d is the Reynolds number based on the cylinder diameter d and free-stream velocity. Large eddy simulation (LES) is conducted for numerical investigation, and direct force and particle image velocimetry (PIV) measurements are conducted for experimental investigation. The drag and base pressure coefficients from present numerical and experimental studies agree well with each other. The instantaneous flow over a circular cylinder exhibits various flow structures such as laminar separation at the cylinder surface, shear-layer after the separation, vivid small-scale vortices and vortex shedding in the wake. In the near wake of circular cylinder, it is observed that a vortical structure distorted in spanwise direction and weak vortex shedding intermittently occurs, inducing relatively low drag and lift fluctuations.

INTRODUCTION

A circular cylinder is a representative bluff body, found in the structures such as wind generator, lamp post, etc. The flow over a circular cylinder at subcritical Reynolds number exhibits various flow phenomena including boundary layer, separation, shear layer evolution and vortex shedding in the wake. Therefore, there have been numerous studies to understand the flow over a circular cylinder experimentally and numerically. However, the experimental results from several researchers show non-negligible variations among themselves (Bearman, 1969; Achenbach and Heinecke, 1981; West and Apelt, 1982; Farell and Blessmann, 1983; Cantwell & Coles, 1983; Szepessy and Bearman, 1992). Furthermore, some attempts were also made to predict the flow around a circular cylinder using large eddy simulation (LES; Fröhlich *et al.*, 1998; Breuer, 2000), but those studies only dealt with the effects of numerics such as grid system, resolution and subgrid-scale models and could not evaluate the prediction performance from numerical simulation due to the scatter in the experimental results. Therefore, in the present study, we investigate the flow over a circular cylinder at a subcritical Reynolds number (Re_d = 140,000) from both the experimental and numerical approaches.

EXPERIMENTAL & COMPUTATIONAL DETAILS

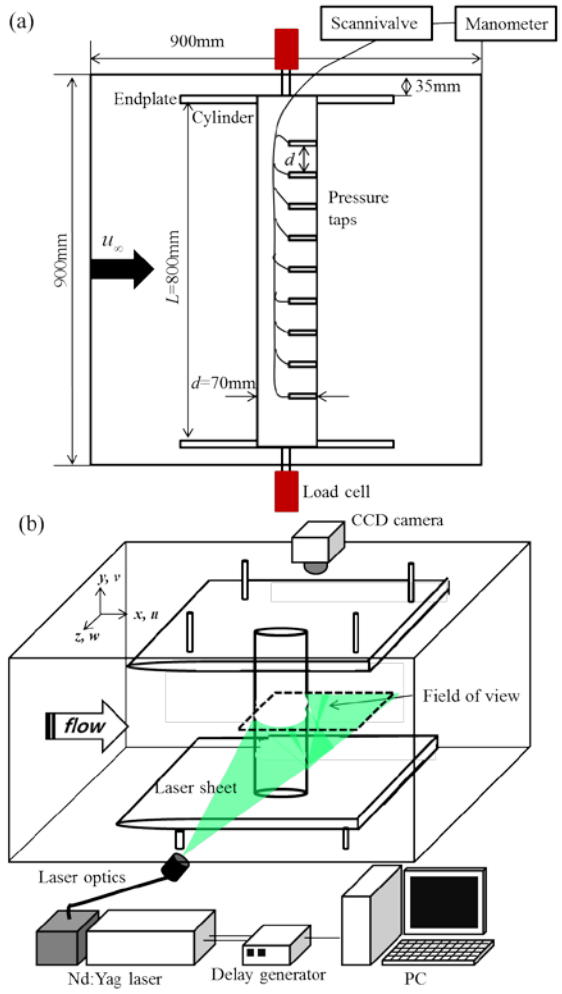

Figure 1. Experimental set-up for (a) force and surface pressure measurements; (b) PIV measurement.

Experimental setup

The present experiment is conducted in a closed-type wind tunnel whose size of test section is 900 mm × 900 mm. The turbulence intensity is lower than 0.3% at the free-stream velocity of 20 m/s. Figure 1a shows the schematic diagram of the present experimental set-up for force and surface pressure measurements, consisting of a circular cylinder, end plate, load cell, pressure holes, scannivalve, and manometer. The cylinder is made of ABS resin with the diameter d = 70 mm. The aspect ratio of the cylinder is 11.4. Boundary-layer thickness on the tunnel-wall is about 25 mm at 20 m/s. The end plate, suggested by Stansby (1974), is installed with the distance 35 mm from the top and bottom of the test section to remove the effect of the boundary layer. The blockage ratio of present setup is 7.8%. Drag force on the cylinder is measured directly using two load cells installed at the both end of cylinder and averaged for 80 seconds. There are nine holes for pressure measurement in the spanwise direction. The distance between pressure holes is 70 mm and each hole is connected directly to the scannivalve with Teflon tube.

The free-stream velocity varies from 20 to 55 m/s, corresponding to the Reynolds numbers based on the free-stream velocity and the cylinder diameter, Re_d = 90,000 – 260,000.

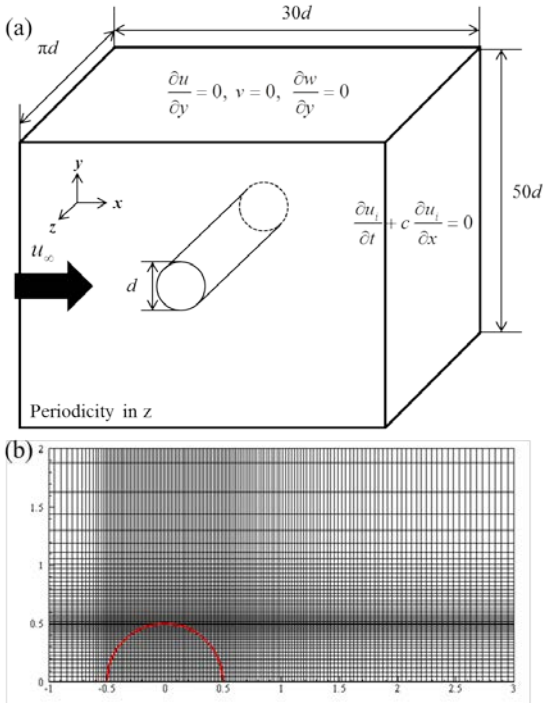

Figure 2. (a) Schemtaic diagram of the computational domain and boundary conditions; (b) typical mesh near circular cylinder. Every 4th grid is shown.

Figure 1b shows the schematic diagram for particle image velocimetry (PIV) measurement. The PIV system consists of a Nd:Yag laser of 120 mJ, a CCD camera of 2048 × 2048 pixels resolution and a delay generator. The velocity measurement is conducted in *xy*-plane at the center of the cylinder span. A 60 mm lens mounted on a digital camera is used to provide a field of view, whose size is 130 mm × 130 mm.

Computational details

In the present study, LES of the flow over a circular cylinder is conducted at Re_d = 140,000. The governing equations of an unsteady incompressible viscous flow for LES are the filtered continuity and Navier-Stokes equations. For the time integration, a fully implicit method based on the Crank-Nicolson method is used. For the spatial discretization, we use a hybrid scheme (Yun *et al.* 2006): a third-order QUICK scheme is used in laminar flow region before separation to prevent the dispersion error caused by the central difference scheme, and the second-order central difference scheme is used elsewhere. The no-slip boundary condition on the cylinder surface is realized by the immersed boundary method by Kim *et al.* (2001) in the Cartesian coordinate system. The subgrid-scale stress for LES is modelled using the dynamic global model (Park *et al.*, 2006; Lee *et al.*, 2010). Figure 2a shows the schematic diagram of computational domain, coordinate system and boundary conditions used in this study. The computational domain is $-15 \le x/d \le 15$, $-25 \le y/d \le 25$, and $0 \le z/d \le \pi$, where x, y, and z denote the streamwise, transve rse, and spanwise directions, respecti-

Table 1. Flow statistics at Re_d = 140,000.

	C_D	C_{Pb}	St
Present (LES)	1.223	-1.30	0.200
Present (experiment)	1.267	-1.36	-
Cantwell and Coles (1983; experiment)	1.237	-1.21	0.179

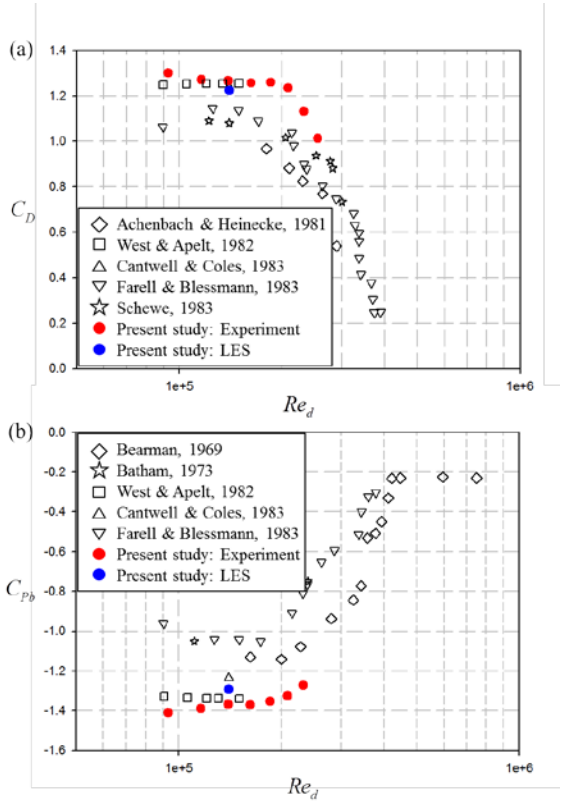

Figure 3. Variations of the drag and base pressure coefficients with the Reynolds number: (a) drag coefficient (C_D); (b) base pressure coefficient (C_{Pb}).

vely. At the inlet, a uniform free-stream velocity condition is imposed. At the outlet, a convective boundary condition is used: $\partial u_i/\partial t + c\partial u_i/\partial x = 0$, where u_i is the velocity, t is the time and c is the mean exit velocity. A Neumann boundary condition is used at the far-field boundaries and periodic boundary condition is used in the spanwise direction. The number of grid points used in present LES is 1041 (x) × 501 (y) × 81 (z). As shown in Figure 2b, the computational mesh for present study is clustered near the boundary of circular cylinder and wake.

RESULTS AND DISCUSSION

Mean flow statistics

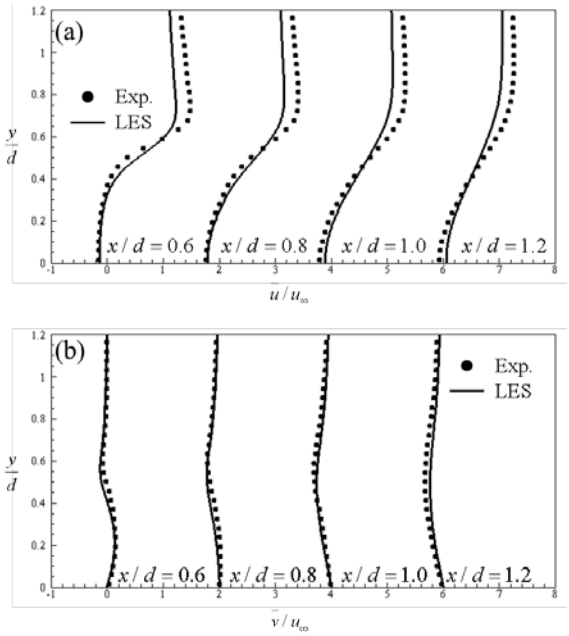

Figure 4. Time-averaged velocity profiles: (a) streamwise velocity; (b) transverse velocity.

Table 1 shows the time-averaged drag coefficient, base pressure coefficient, and Strouhal number at Re_d = 140,000 from present LES and experiment together with those from previous experimental work (Cantwell and Coles, 1983). In the present LES, the statistics are averaged over about $210d/u_\infty$ (about 42 vortex shedding cycles), after the initial transient period. In the present experiment, the base pressure coefficients at nine spanwise positions are measured and their variations from the averaged value are within 3%, indicating that the flow over a circular cylinder is nominally two-dimensional. While obtaining the drag and base pressure coefficients in the present experiment, a correction method suggested by Allen and Vincenti (1944) is applied to compensate the blockage effect. As shown in Table 1, the statistics from the present LES and experiment agree well with each other, and are also in good agreements with those from previous experimental data.

Figure 3 shows the variations of the drag and base pressure coefficients with the Reynolds number. Both the drag and base pressure coefficients from present experiment remain almost constant at the subcritical Reynolds number range (Re_d < 200,000). The drag and base pressure coefficients from present study show good agreements with those of West and Apelt (1982), but they are quite different from those of Farell and Blessmann (1983). This may be attributed to the fact that end plates were absent in the experiment of Farell and Blessmann (1983), and this allowed developing boundary layer on the tunnel-wall to affect flow over a circular cylinder (Fox and West, 1990).

Figure 4 shows the time-averaged streamwise and transverse velocity profiles at four streamwise positions behind the cylinder obtained from the present LES and experiment. In Figure 4a, the streamwise velocity profiles from present LES and experiment are overall in good agreement with each other while those of present LES are slightly underpredicted at y/d > 0.6 compared to those of

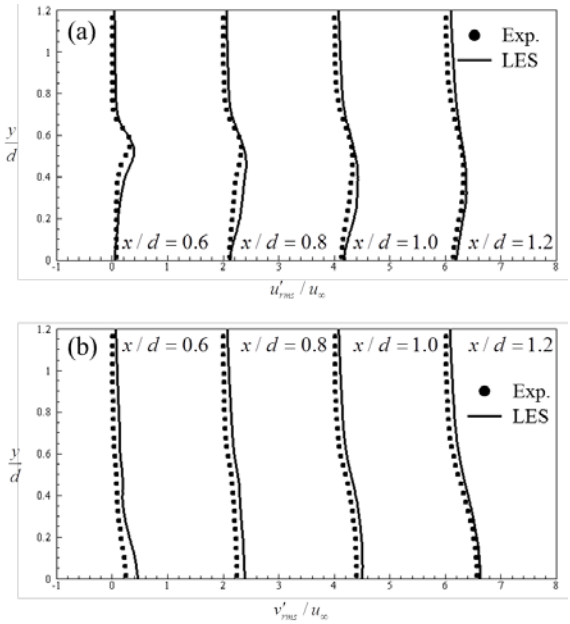

Figure 5. Profiles of root-mean-square (rms) velocity fluctuations: (a) streamwise velocity fluctuations; (b) transverse velocity fluctuations.

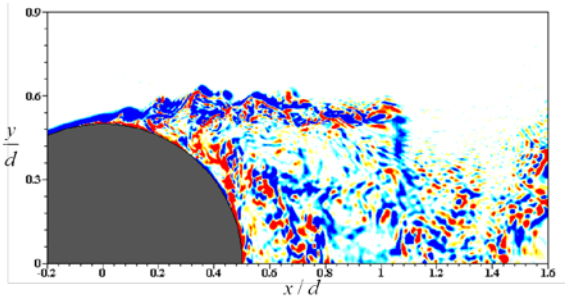

Figure 6. Contours of the instantaneous spanwise vorticity near circular cylinder. The contour levels are from -20 to 20 with increments of 2.

experiment. On the other hand, in Figure 4b, the transverse velocity profiles from present experiment and LES show excellent agreements with each other.

Figure 5 shows the profiles of root-mean-square (rms) streamwise and transverse velocity fluctuations at four streamwise locations behind the cylinder. At all locations, results from LES are in good agreements with those from experiment.

Instantaneous flow field

Figure 6 shows the contours of instantaneous spanwise vorticity in an *xy*-plane near the cylinder surface. As shown, right after the laminar separation at about 83°, the shear-layer instability occurs and small-scale vortices roll up.

Figure 7a shows the temporal variations of drag and lift coefficient from present LES. In the figure, A and B represent instances where the low and high drag/lift-fluctuations occur, respectively. To examine the flow structures at the instances of A and B, instantaneous large-

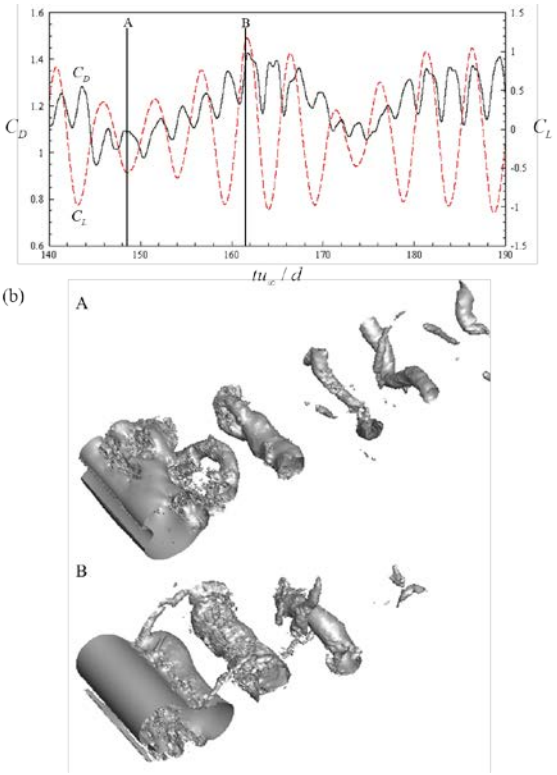

Figure 7. LES results at Re_d = 140,000: (a) temporal variations of drag and lift coefficients; (b) instantaneous vortical structures identified by iso-surface of pressure (p = -0.3).

scale vortical structures identified by the iso-surface of pressure are shown in Figure 7b. At the instance of A, the vortical structure near the cylinder is distorted along the spanwise direction and the vortex shedding is relatively weak. The low drag and lift fluctuations at the instance of A may be attributed to this weak vortical structure in the wake (Choi *et al.*, 2008). On the other hand, at the instance of B, the variation of vortical structure in spanwise direction is small, indicating that it is nominally two-dimensional, and the vortex shedding in the wake is strong. This behaviour of vortical structure is responsible for high drag and lift fluctuations at the instance of B.

CONCLUSIONS

In the present study, flow over a circular cylinder at Re_d = 140,000 was investigated through numerical simulation and experiment. The flow statistics from LES such as drag coefficient, base pressure coefficient, and profiles of mean velocity and rms velocity fluctuations in the near wake showed good agreements with the present and previous experimental data. The instantaneous flow over a circular cylinder exhibited various flow structures such as laminar separation at the cylinder surface, shear-layer after the separation, vivid small-scale vortices and vortex shedding in the wake. In the near wake of circular cylinder, it was observed that a vortical structure distorted in spanwise direction and weak vortex shedding

intermittently occurred, inducing relatively low drag and lift fluctuations.

ACKNOWLEDGEMENT

The authors would like to acknowledge the supports from KISTI (Korea Institute of Science and Technology Information) under "The Strategic Supercomputing Support Program" and NRF program (20120008740).

REFERENCES

Achenbach, H., and Heinecke, E., 1981, "On vortex shedding from smooth and rough cylinders in the range of Reynolds numbers 6×10^3 to 5×10^6", *J. Fluid Mech*., Vol. 109, pp. 239-251.

Allen, H. J., and Vincenti, W. G., 1944, "Wall interference in a two-dimensional-flow wind tunnel, with consideration of the effect of compressibility", *N.A.C.A. Rep*. no. 782.

Batham, J. P., 1973, "Pressure distributions on circular cylinders at critical Reynolds numbers", *J. Fluid Mech*., Vol. 57, Part 2, pp. 209-228.

Bearman, P. W., 1969, "On vortex shedding from a circular cylinder in the critical Reynolds number regime", *J. Fluid Mech.*, Vol. 37, pp. 577-585.

Breuer, M., 2000, "A challenging test case for large eddy simulation: high Reynolds number circular cylinder flow", *Int'l J. Heat and Fluid Flow*, Vol. 21, pp. 648-654.

Cantwell, B., and Coles, D., 1983, "An experimental study of entrainment and transport in the turbulent near wake of a circular cylinder", *J. Fluid Mech*., Vol. 136, pp. 321-374.

Choi, H., Jeon, W.-P., and Kim, J., 2008, "Control of flow over a bluff body", *Annu. Rev. Fluid Mech*., Vol. 40, pp. 113-139.

Farell, C., and Blessmann, J., 1983, "On critical flow around smooth circular cylinders", *J. Fluid Mech*., Vol. 136, pp. 375-391.

Fox, T. A., and West, G. S., 1990, "On the use of end plates with circular cylinders", *Exp. Fluids*, Vol. 9, pp. 237-239.

Fröhlich, J., Rodi, W., Kessler, Ph., Parpais, S., Bertoglio, J. P., and Laurence, D., 1998, "Large eddy simulation of flow around circular cylinders on structured and unstructured grids", *Notes on Numerical Fluid Mechanics*, Vol. 66, pp.319-338.

Kim, J., Kim, D., and Choi, H., 2001, "An immersed-boundary finite volume method for simulations of flow in complex geometries", *J. Comp. Phys*., Vol. 171, pp. 132-150.

Lee, J., Choi, H., and Park, N., 2010, "Dynamic global model for large eddy simulation of transient flow", *Phys. Fluids*, Vol. 22, 075106.

Park, N., Lee, S., Lee, J., and Choi, H., 2006, "A dynamic subgrid-scale eddy-viscosity model with a global model coefficient", *Phys. Fluids*, Vol. 18, 125109.

Schewe, G., 1983, "On the force fluctuations acting on a circular cylinder in crossflow from subcritical up to transcritical Reynolds numbers", *J. Fluid Mech*., Vol. 133, pp. 265-285.

Stansby, P. K., 1974, "The effects of end plates on the base pressure coefficient of a circular cylinder", *Aeronautical Journal*, Vol. 78, pp. 36-37.

West, G. S., and Apelt, C. J., 1982, "The effects of tunnel blockage and aspect ratio on the mean flow past a circular cylinder with Reynolds numbers between 10^4 and 10^5", *J. Fluid Mech*., Vol. 114, pp. 361-377.

Yun, G., Kim, D., and Choi, H., 2006, "Vortical structures behind a sphere at subcritical Reynolds numbers", *Phys. Fluids*, Vol. 18, 015102.